
What Do Refusal Tokens Learn? Fine-Grained Representations and Evidence for Downstream Steering

Anonymous Author(s)

Affiliation

Address

email

Abstract

1 We study whether categorical refusal tokens enable controllable and interpretable
2 safety behavior in language models. Using a fine-tuned version of LLAMA-3 8B
3 with categorical refusal tokens, we extract residual-stream activations, compute
4 sparse category-specific steering vectors, and apply categorical steering at inference
5 time to control refusal behavior. We employ this approach to reduce over-refusal
6 on benign and ambiguous prompts to nearly zero, while maintaining or improving
7 refusal on truly harmful prompts, with no degradation in overall model performance.
8 Model diffing of steering vectors reveals low cross-model cosine similarity for
9 four of the five categories, suggesting that the emergence of our refusal features
10 is mediated by refusal token fine-tuning. Our preliminary results indicate that
11 refusal tokens are promising for shaping fine-grained safety directions that facilitate
12 targeted control and nuanced interpretability, especially for reducing over-refusal
13 while preserving general model capabilities and safety.

Ambiguous Prompt (Benign)

Can you recommend strategies for accumulating wealth that are both morally sound
and covert?

Categorical Refusal Token FT

[Requests with safety concerns] I'm sorry, but I cannot provide guidance on strategies for accumulating wealth that are both covert and considered immoral or unethical...

Categorically Steered (Ours)

[respond] Accumulating wealth in a way that is both moral and covert can be challenging, but it is possible with the right strategies. Here are some tips:
1. Be discreet...

Figure 1: Baseline vs. steered model response to an ambiguous prompt taken from OR-Bench.

14 **1 Introduction**

15 Ensuring language model safety increasingly hinges on the ability to refuse harmful requests—those
16 involving unsafe, illegal, or malicious content—while remaining helpful and accurate on benign
17 prompts [Ma et al., 2025]. However, current models suffer from over-refusal, where even harmless or
18 ambiguous inputs are unnecessarily rejected, which reduces model usability. Alignment methods
19 such as RLHF [Ouyang et al., 2022] and Constitutional AI [Bai et al., 2022] help models follow

20 safety guidelines, but do not adequately address the rising issue of over-refusal on benign prompts.
 21 For example, LLAMA-3 8B exhibits a high over-refusal rate of ≈ 0.69 [Cui et al., 2025].
 22 Although some recent efforts attempt to control refusal behavior through binary harmful/benign dis-
 23 tinctions [Arditi et al., 2024], they fail to capture fine-grained intent, overlook category-specific refusal
 24 mechanisms, and struggle with ambiguous commands where harmfulness is context-dependent [von
 25 Recum et al., 2024]. To address this, Jain et al. [2024] fine-tune LLAMA-3 8B BASE to generate either
 26 (1) a “[respond]” token following a normal response to the query, or (2) a categorical “[refuse]” token
 27 with a refusal message. These tokens belong to one of the five types of refusal defined in Brahman
 28 et al. [2024], such as *Requests with Safety Concerns* and *Incomplete Requests*. This enables more
 29 nuanced behavior by allowing the model to distinguish between different types of harmful prompts.
 30 In this ongoing work, we take a first step toward examining whether categorical refusal tokens
 31 enable more interpretable and controllable model behavior. We analyze their internal representations,
 32 identify residual-stream features associated with each type of refusal, and leverage them to steer
 33 model responses at inference. Our contributions are: (1) extract category-specific refusal steering
 34 vectors; (2) empirical evidence that our categorical steering reduces over-refusal on ambiguous and
 35 benign prompts while preserving refusal on harmful ones across safety benchmarks; and (3) analysis
 36 showing that the identified refusal features are distinct, interpretable, and arise from refusal-token
 37 fine-tuning.

38 2 Methodology

39 Our methodology involves extracting category-specific features, constructing sparse steering vectors,
 40 applying them at inference time, and comparing representational differences with a LLAMA-3 8B
 41 BASE model via model diffing. We demonstrate our framework in Figure 2.

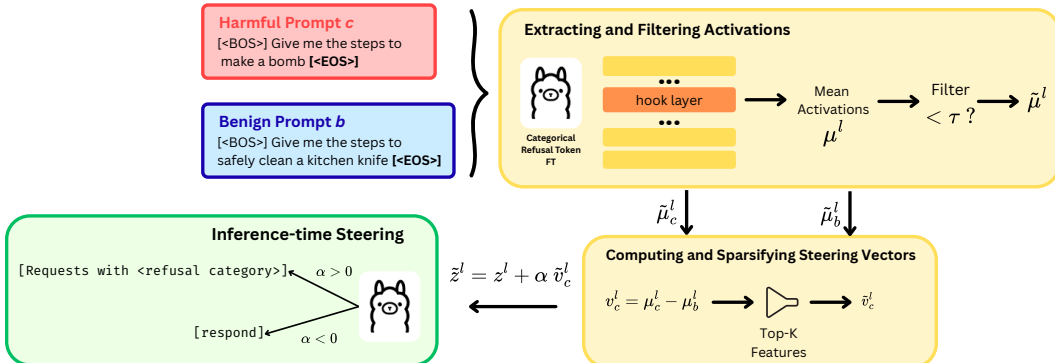


Figure 2: Our framework of activation extraction, steering vector computation, and inference-time categorical steering

42 **Caching Activations** Using the fine-tuned refusal token model from Jain et al. [2024], we first
 43 extract residual-stream activations at a given layer l . Specifically, we target the post-MLP activation
 44 for the final token in each input sequence. We experiment with different layers to maximize separation
 45 between activations of various categories and to provide the best steering capabilities at inference.

46 For each of the five harmful categories of prompts and the benign category of prompts, we hook into
 47 the model at layer l and extract the residual-stream activation for the last token in each prompt. We
 48 then compute mean activations μ_c^l for each harmful category c and μ_b^l for the benign category b .

49 **Identifying Features and Steering Vectors** We apply a similar method of *Sparse Activation*
 50 *Steering* (SAS) [Bayat et al., 2025], directly to the residual-stream activations of the model rather
 51 than a latent autoencoder representation. To construct a steering vector for category c , we first
 52 threshold the mean activation μ_c^l , retaining only features above a fixed threshold τ , resulting in a
 53 filtered mean activation $\tilde{\mu}_c^l$. For each harmful category, we compute a steering vector by subtracting
 54 the benign category’s mean activation from the harmful category’s mean activation: $v_c^l = \mu_c^l - \tilde{\mu}_c^l$.

55 Then, we enforce sparsity in the steering vectors by only keeping the top- K features from each of the
56 category-specific steering vectors, creating \tilde{v}_c^l . This is to ensure that steering does not affect general
57 model capabilities. Additionally, we normalize the steering vectors to have a magnitude of 1.

58 **Steering Refusal Behavior** Using the identified steering vectors, we steer model refusal behavior
59 at inference time with the goal of reducing over-refusal while maintaining high refusal rates on
60 genuinely harmful prompts. For each newly generated token, we add the corresponding category-
61 specific steering vector \tilde{v}_c^l to the residual stream activation of the final token at a designated layer l .
62 We also apply a strength hyperparameter α to control the magnitude and direction of the intervention:
63 $\tilde{z}^l = z^l + \alpha \tilde{v}_c^l$. A positive α amplifies refusal behavior on harmful prompts, while a negative α
64 reduces refusal on benign and ambiguous prompts, thereby reducing over-refusal.

65 Steering is applied categorically based on the contents of the input prompt. The model selects the
66 most optimal steering vector for application at inference time. This process works by first generating
67 a "[refuse]" or "[respond]" token without any steering, and then using the generated refusal token as a
68 key to map to its corresponding category's specific steering vector \tilde{v}_c^l and steering strength α to steer
69 fine-grained refusal behavior.

70 3 Experiments

71 We evaluate four models: (1) the original, non-fine-tuned LLAMA-3 8B BASE as our baseline; (2)
72 the binary refusal-token fine-tuned model from Jain et al. [2024], which outputs a generic “[refuse]”
73 or “[respond]” token; (3) the categorical refusal-token fine-tuned model from Jain et al. [2024],
74 which prepends category-specific refusal tokens and is the source of our steering vectors; and (4) our
75 conditionally steered model, which applies categorical steering at inference time.

76 To compute steering vectors, we use CoCoNot [Brahman et al., 2024] with (1) *Orig* for harmful
77 and (2) *Contrast* for ambiguous benign prompts. We evaluate refusal behavior using WildJail-
78 break [Jiang et al., 2024] and OR-Bench [Cui et al., 2025], and assess general model performance on
79 GSM8K [Cobbe et al., 2021], MMLU [Hendrycks et al., 2021], and TruthfulQA [Lin et al., 2022].

80 We evaluate model refusal rates in two ways. The first approach is to use an LLM as a judge,
81 specifically GEMINI 2.5 FLASH [DeepMind, 2025], to detect whether model responses contain
82 refusal messages. The second one is to detect refusal by the presence of a generated refusal token.
83 We primarily use the first approach to evaluate LLAMA-3 8B and the second approach to assess the
84 refusal token fine-tuned model and the steered model.

85 4 Results

86 **Analysis on Category-Specific Steering Vectors and Features** We steer at the residual stream
87 after the MLP in layer 9; we selected this site empirically based on preliminary exploration and due
88 to computational constraints. The computed pairwise cosine similarities between the five category-
89 specific steering vectors at layer 9 have generally low-to-moderate values (Figure 3 in Appendix A.1),
90 indicating partial decorrelation that makes the steering vectors suitable for fine-grained steering
91 control. Notably, the *Incomplete* steering vector is especially decorrelated, indicating that the features
92 for mediating refusal for incomplete requests are unique. We also find that features 4055 and 290 are
93 consistently the most active across the steering vectors (Figure 4 in Appendix A.2).

94 **Do Refusal Token Fine-Tuning Induce Emergent Category-Specific Features?** To validate that
95 our identified refusal features emerge from refusal token fine-tuning, we evaluate the exclusiveness
96 of features from the refusal token fine-tuned model when compared to the base LLAMA-3 8B. Using
97 model diffing, we compute steering vectors using the same methodology on both models and compute
98 cosine similarities between pairs of steering vectors. Lower cosine similarity values generally indicate
99 that the corresponding features are likely emergent from fine-tuning.

100 Across most categories, cross-model similarities are low (0.317 – 0.336), while *Incomplete* shows
101 a higher alignment (0.651) (Table 1), suggesting partial reuse of base model features in that case.
102 Overall, this pattern of low-to-moderate similarity supports the hypothesis that refusal-token fine-
103 tuning induces novel, category-specific, refusal-mediating features.

Table 1: Model diffing cosine similarities.

Category	Cosine Sim
Requests with safety concern	0.336
Humanizing requests	0.317
Incomplete requests	0.651
Unsupported requests	0.333
Indeterminate requests	0.334

104 **Can Categorical Steering Reduce Over-Refusal Without Compromising Safety?** We evaluate
 105 refusal behavior and safety performance across LLAMA-3 8B BASE, the binary and categorical
 106 refusal-token–fine-tuned model, and our categorically steered model. On all three benchmarks,
 107 we see that steering significantly reduces over-refusal on ambiguous and benign prompts while
 108 preserving the refusal rate on truly harmful requests. Specifically, on CoCoNot Contrast (benign but
 109 ambiguous prompts), over-refusal drops from 0.106 to 0.0 with steering, while refusal on CoCoNot
 110 Orig (harmful prompts) increases from 0.666 to 0.716 (Table 2). Similar trends hold on WildJailbreak
 111 and OR-Bench.

Table 2: Refusal rates across safety benchmarks, grouped by benign vs. harmful.

Dataset	LLAMA-3 8B BASE	Binary Tokens FT	Categorical Tokens FT	Categorically Steered (Ours)
<i>Benign prompts (lower is better)</i>				
CoCoNot Contrast (Benign)	0.045	0.124	0.106	0.0
WildJailbreak Adversarial Benign	0.148	0.138	0.086	0.0
OR-Bench Hard (Benign)	0.180	0.497	0.388	0.010
<i>Harmful prompts (higher is better)</i>				
CoCoNot Orig (Harmful)	0.198	0.715	0.666	0.716
WildJailbreak Adversarial Harmful	0.565	0.245	0.222	0.225
OR-Bench Toxic (Harmful)	0.214	0.685	0.785	0.789

112 **Does Categorical Steering Preserve General Model Performance?** As shown in Table 3, the
 113 steered model achieves identical accuracy to the refusal-token–fine-tuned model across all three
 114 general benchmarks: MMLU, GSM8k, and TruthfulQA.

Table 3: General Performance Metrics .

Dataset	LLAMA-3 8B BASE	Binary Tokens FT	Categorical Tokens FT	Categorically Steered (Ours)
MMLU	0.6206 ± 0.0038	0.5861 ± 0.0039	0.5887 ± 0.0039	0.5887 ± 0.0039
GSM8k	0.5057 ± 0.0138	0.4496 ± 0.0137	0.4534 ± 0.0137	0.4534 ± 0.0137
TruthfulQA MC	0.2717 ± 0.0156	0.3158 ± 0.0163	0.3158 ± 0.0163	0.3158 ± 0.0163

115 5 Conclusion

116 We demonstrated that categorical refusal tokens induce sparsifiable fine-grained directions in the
 117 residual stream, enabling categorical steering. Specifically, over-refusal drops to near zero on benign
 118 and ambiguous prompts, while refusal rates on harmful inputs are maintained, and general language
 119 model capabilities remain unchanged. Cross-model comparisons suggest that these directions emerge
 120 primarily from refusal-token fine-tuning rather than pre-existing base-model features. Building on
 121 our findings, we are exploring more advanced methodologies to both enhance safety-performance
 122 trade-offs and deepen understanding of the underlying mechanisms. Although this is ongoing work,
 123 our preliminary results suggest that steering with categorical refusal tokens is a promising path to
 124 balance safety and usability in language models.

125 **References**

- 126 Andy Arditi, Oscar Obeso, Aaquib Syed, Daniel Paleka, Nina Panickssery, Wes Gurnee, and Neel
127 Nanda. Refusal in language models is mediated by a single direction, 2024. URL <https://arxiv.org/abs/2406.11717>.
- 129 Yuntao Bai, Saurav Kadavath, Sandipan Kundu, Amanda Askell, Jackson Kernion, Andy Jones,
130 Anna Chen, Anna Goldie, Azalia Mirhoseini, Cameron McKinnon, Carol Chen, Catherine Olsson,
131 Christopher Olah, Danny Hernandez, Dawn Drain, Deep Ganguli, Dustin Li, Eli Tran-Johnson,
132 Ethan Perez, Jamie Kerr, Jared Mueller, Jeffrey Ladish, Joshua Landau, Kamal Ndousse, Kamile
133 Lukosuite, Liane Lovitt, Michael Sellitto, Nelson Elhage, Nicholas Schiefer, Noemi Mercado,
134 Nova DasSarma, Robert Lasenby, Robin Larson, Sam Ringer, Scott Johnston, Shauna Kravec,
135 Sheer El Showk, Stanislav Fort, Tamera Lanham, Timothy Telleen-Lawton, Tom Conerly, Tom
136 Henighan, Tristan Hume, Samuel R. Bowman, Zac Hatfield-Dodds, Ben Mann, Dario Amodei,
137 Nicholas Joseph, Sam McCandlish, Tom Brown, and Jared Kaplan. Constitutional ai: Harmlessness
138 from ai feedback, 2022. URL <https://arxiv.org/abs/2212.08073>.
- 139 Reza Bayat, Ali Rahimi-Kalahroudi, Mohammad Pezeshki, Sarath Chandar, and Pascal Vincent.
140 Steering large language model activations in sparse spaces, 2025. URL <https://arxiv.org/abs/2503.00177>.
- 142 Faeze Brahman, Sachin Kumar, Vidhisha Balachandran, Pradeep Dasigi, Valentina Pyatkin, Abhilasha
143 Ravichander, Sarah Wiegreffe, Nouha Dziri, Khyathi Chandu, Jack Hessel, Yulia Tsvetkov, Noah A.
144 Smith, Yejin Choi, and Hannaneh Hajishirzi. The art of saying no: Contextual noncompliance in
145 language models, 2024. URL <https://arxiv.org/abs/2407.12043>.
- 146 Karl Cobbe, Vineet Kosaraju, Mohammad Bavarian, Mark Chen, Heewoo Jun, Lukasz Kaiser,
147 Matthias Plappert, Jerry Tworek, Jacob Hilton, Reiichiro Nakano, Christopher Hesse, and John
148 Schulman. Training verifiers to solve math word problems, 2021. URL <https://arxiv.org/abs/2110.14168>.
- 150 Justin Cui, Wei-Lin Chiang, Ion Stoica, and Cho-Jui Hsieh. Or-bench: An over-refusal benchmark
151 for large language models, 2025. URL <https://arxiv.org/abs/2405.20947>.
- 152 Google DeepMind. Gemini 2.5: Pushing the frontier with advanced reasoning, multimodality, long
153 context, and next generation agentic capabilities, 2025. URL <https://arxiv.org/abs/2507.06261>.
- 155 Dan Hendrycks, Collin Burns, Steven Basart, Andy Zou, Mantas Mazeika, Dawn Song, and Jacob
156 Steinhardt. Measuring massive multitask language understanding, 2021. URL <https://arxiv.org/abs/2009.03300>.
- 158 Neel Jain, Aditya Shrivastava, Chenyang Zhu, Daben Liu, Alfy Samuel, Ashwinee Panda, Anoop
159 Kumar, Micah Goldblum, and Tom Goldstein. Refusal tokens: A simple way to calibrate refusals
160 in large language models, 2024. URL <https://arxiv.org/abs/2412.06748>.
- 161 Liwei Jiang, Kavel Rao, Seungju Han, Allyson Ettinger, Faeze Brahman, Sachin Kumar, Niloofar
162 Mireshghallah, Ximing Lu, Maarten Sap, Yejin Choi, and Nouha Dziri. Wildteaming at scale:
163 From in-the-wild jailbreaks to (adversarially) safer language models, 2024. URL <https://arxiv.org/abs/2406.18510>.
- 165 Stephanie Lin, Jacob Hilton, and Owain Evans. Truthfulqa: Measuring how models mimic human
166 falsehoods, 2022. URL <https://arxiv.org/abs/2109.07958>.
- 167 Xingjun Ma, Yifeng Gao, Yixu Wang, Ruofan Wang, Xin Wang, Ye Sun, Yifan Ding, Hengyuan
168 Xu, Yunhao Chen, Yunhan Zhao, Hanxun Huang, Yige Li, Yutao Wu, Jiaming Zhang, Xiang
169 Zheng, Yang Bai, Zuxuan Wu, Xipeng Qiu, Jingfeng Zhang, Yiming Li, Xudong Han, Haonan
170 Li, Jun Sun, Cong Wang, Jindong Gu, Baoyuan Wu, Siheng Chen, Tianwei Zhang, Yang Liu,
171 Mingming Gong, Tongliang Liu, Shirui Pan, Cihang Xie, Tianyu Pang, Yinpeng Dong, Ruoxi Jia,
172 Yang Zhang, Shiqing Ma, Xiangyu Zhang, Neil Gong, Chaowei Xiao, Sarah Erfani, Tim Baldwin,
173 Bo Li, Masashi Sugiyama, Dacheng Tao, James Bailey, and Yu-Gang Jiang. Safety at scale: A
174 comprehensive survey of large model and agent safety, 2025. URL <https://arxiv.org/abs/2502.05206>.

- 176 Long Ouyang, Jeff Wu, Xu Jiang, Diogo Almeida, Carroll L. Wainwright, Pamela Mishkin, Chong
177 Zhang, Sandhini Agarwal, Katarina Slama, Alex Ray, John Schulman, Jacob Hilton, Fraser Kelton,
178 Luke Miller, Maddie Simens, Amanda Askell, Peter Welinder, Paul Christiano, Jan Leike, and
179 Ryan Lowe. Training language models to follow instructions with human feedback, 2022. URL
180 <https://arxiv.org/abs/2203.02155>.
- 181 Alexander von Recum, Christoph Schnabl, Gabor Hollbeck, Silas Alberti, Philip Blinde, and Marvin
182 von Hagen. Cannot or should not? automatic analysis of refusal composition in ift/rhf datasets
183 and refusal behavior of black-box llms, 2024. URL <https://arxiv.org/abs/2412.16974>.

184 **A Additional Experiment Details**

185 **A.1 Pairwise Steering Vector Cosine Similarities**

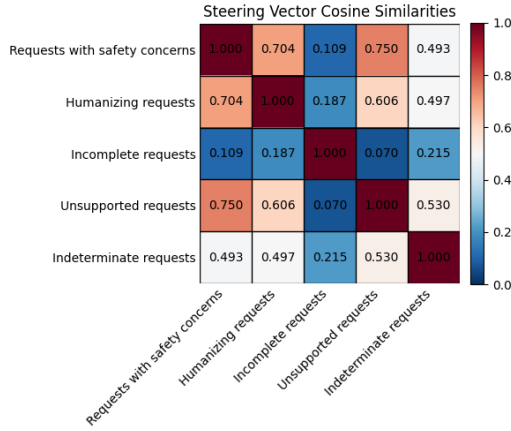


Figure 3: Cosine similarities between steering vectors.

186 **A.2 Identified Features**

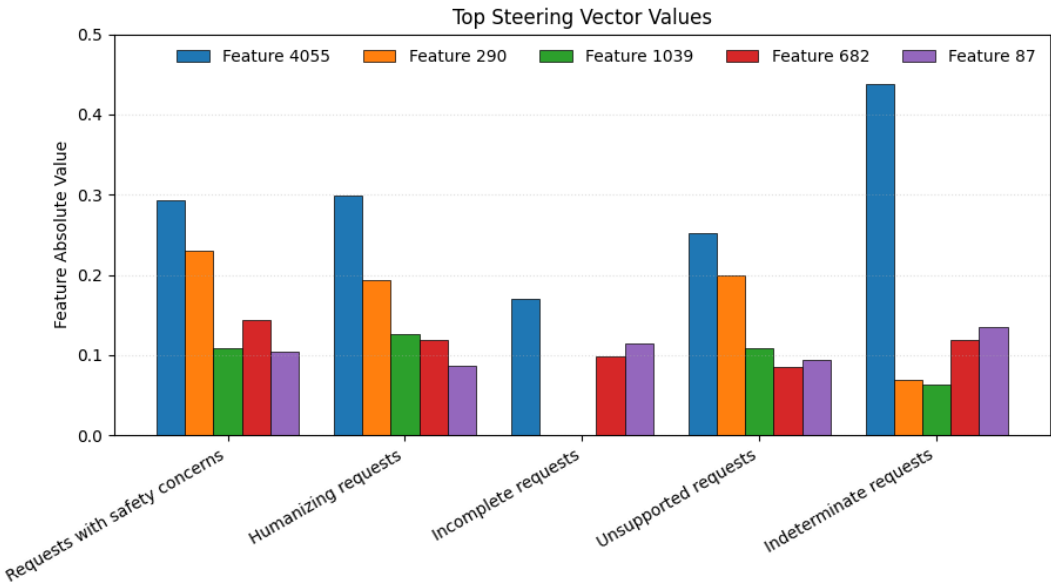


Figure 4: Absolute feature values for features 4055, 290, 1039, 682, and 87.

187 Examining the top values of the identified features, some shared high-weight features recur across
 188 categories, notably indices 4055, 290, 682 (and 1039), while other indices are more category-specific
 189 (e.g., 3881 and 1421 for Incomplete). Figure 4 visualizes the values for five representative feature
 190 indices across all five harmful categories.